

# Quasi-particle perspective on QCD matter and critical end point effects

Marcus Bluhm<sup>1</sup> and Burkhard Kämpfer<sup>1,2</sup>

<sup>1</sup> Institut für Kern- und Hadronenphysik, Forschungszentrum Rossendorf, PF 510119, 01314 Dresden, Germany

<sup>2</sup> Institut für Theoretische Physik, TU Dresden, 01062 Dresden, Germany

## Abstract

Our quasi-particle model is compared with recent lattice QCD data at finite temperature and baryon number density with emphasis on the coefficients in the Taylor series expansion of thermodynamic observables. The inclusion of static critical end point effects into the equation of state is discussed.

## 1 Introduction

The QCD phase diagram exhibits an astonishingly rich phase structure. The (pseudo-) critical line, which separates the phase dominated by quark and gluon degrees of freedom at large temperature  $T$  and baryo-chemical potential  $\mu_B$  from the one dominated by hadrons and resonances, has been investigated by means of lattice gauge theory [1, 2, 3, 4]. From theoretical reasoning [5, 6] for finite quark masses, the phase transition is of first order at finite  $T$  and large  $\mu_B$  ending in a critical point of second order. For smaller  $\mu_B$ , thermodynamic observables change rapidly but continuously indicating a crossover regime. There, the equation of state (EoS) has been computed for  $N_f = 2$  quark flavours [7, 8]. While the location of the critical end point (CEP) showing a strong quark mass dependence [3, 9] was determined by first principle QCD evaluations [4, 10], the extension of the critical region is fairly unknown. Lattice QCD studies of the volume dependence of the Binder cumulant [3, 11] indicate that the CEP belongs to the static universality class of the 3D Ising model. At present, many investigations aim to study implications of such a fundamental issue of QCD. In particular, observable consequences of the occurrence of the CEP as novel feature of QCD are discussed [12]. Heaving in mind the successful hydrodynamical description of the expansion stage in heavy-ion collisions, one intriguing problem concerns the manner the EoS of strongly interacting matter becomes modified by the CEP. This is the subject of the present contribution.

In 2, the quasi-particle model is shortly reviewed and compared with recent lattice QCD results. We focus on the Taylor series expansion coefficients [7, 8]. In 3, CEP effects on the EoS are discussed for a toy model and for our QCD based quasi-particle model. The results are summarized in 4.

## 2 Taylor series expansion of the EoS

Thermodynamic observables can be expressed as Taylor series expansions in powers of  $\mu_B/T$ . Accordingly, the pressure is decomposed into

$$p(T, \mu_B) = T^4 \sum_{n=0}^{\infty} c_{2n}(T) \left( \frac{\mu_B}{3T} \right)^{2n}, \quad (1)$$

where  $c_0(T) = p(T, \mu = 0)/T^4$  and  $c_k(T) = \partial^k p / \partial \mu^k \big|_{\mu=0} T^{k-4}/k!$  with  $\mu = \mu_B/3$ . In [7, 8], the Taylor expansion coefficients up to  $c_6(T)$  have been presented basing on first principle QCD evaluations.

Achieving a flexible parametrization of the EoS, we formulated a model which describes the quark-gluon fluid in terms of quasi-particle excitations [13, 14]

$$p(T, \mu) = \sum_{i=q,g} p_i(T, \mu) - B(T, \mu). \quad (2)$$

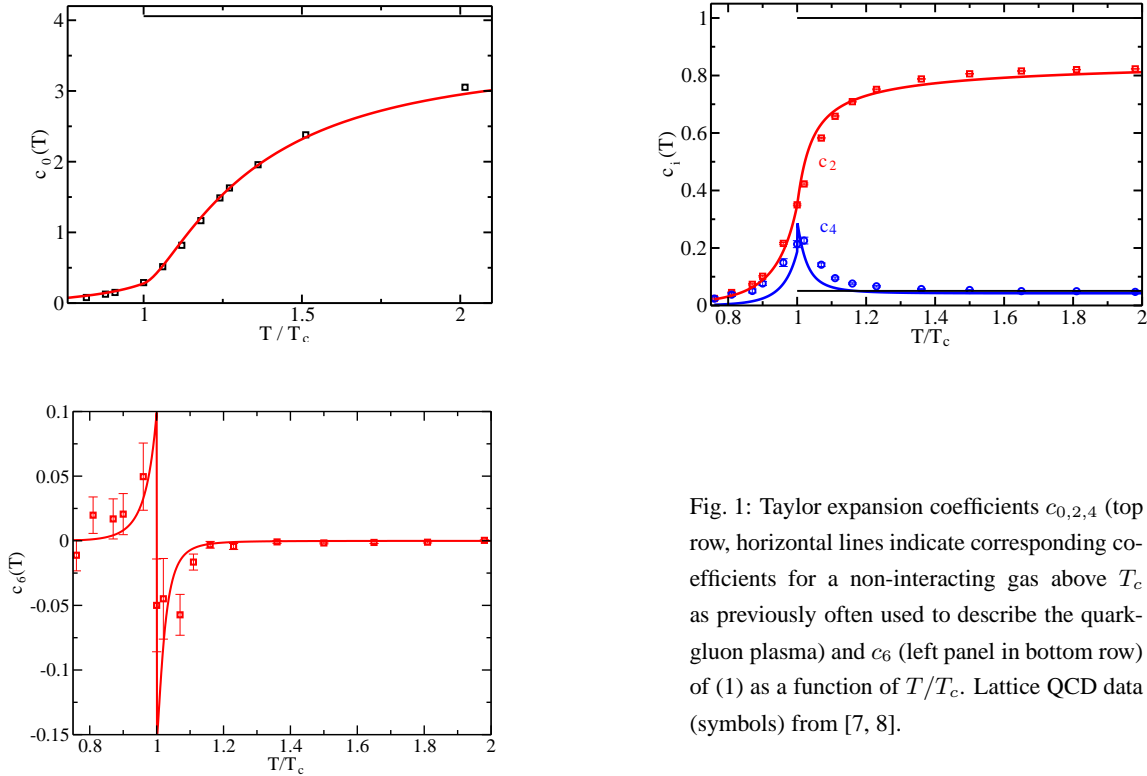


Fig. 1: Taylor expansion coefficients  $c_{0,2,4}$  (top row, horizontal lines indicate corresponding coefficients for a non-interacting gas above  $T_c$  as previously often used to describe the quark-gluon plasma) and  $c_6$  (left panel in bottom row) of (1) as a function of  $T/T_c$ . Lattice QCD data (symbols) from [7, 8].

Here,  $p_i$  denote thermodynamic standard expressions for quarks and transverse gluons with dynamically generated self-energies  $\Pi_i$  and a non-perturbative effective coupling  $G^2(T, \mu)$  as essential input. Thermodynamic self-consistency is ensured through the stationarity conditions  $\delta p / \delta \Pi_i = 0$ , imposing in turn conditions onto  $B(T, \mu)$ . From Maxwell's relation for  $p$ , a flow equation for  $G^2(T, \mu)$  follows [13]

$$a_\mu \frac{\partial G^2}{\partial \mu} + a_T \frac{\partial G^2}{\partial T} = b. \quad (3)$$

Knowing  $G^2$  on an arbitrary curve in the  $T - \mu$  plane, (3) can be solved as a Cauchy problem. For convenience, we adjust  $G^2(T, \mu = 0)$  to lattice data at  $\mu = 0$  enabling a mapping into the finite chemical potential region via (3). The Taylor expansion coefficients follow straightforwardly from (2) as integral expressions involving  $G^2$  and higher order derivatives of the effective coupling at vanishing chemical potential. The latter can be computed by exploiting the flow equation (3) (cf. [14] for details). In Fig. 1, a fairly good agreement between Taylor expansion coefficients from the quasi-particle model and lattice results is shown. In particular, the peak in  $c_4(T)$  and the dipole structure in  $c_6(T)$  are reproduced. Adjusting the parametrization of the effective coupling onto  $c_0(T)$  dictates a change in  $G^2(T, \mu = 0)$  at  $T_c = 170$  MeV from a regularized logarithmic dependence (resembling the perturbative behaviour at large  $T$ ) into a linear dependence. This change in the curvature of  $G^2$  can be considered as implemented phase transition and is responsible for the pronounced structures in  $c_{4,6}(T)$ . In fact, these structures disappear when neglecting higher order derivatives of the effective coupling in the integral expressions of  $c_{4,6}(T)$  serving for a test of the flow equation (3).

### 3 Critical end point

Starting from a thermodynamic potential, e. g. Gibbs free enthalpy, it can be decomposed into an analytic and a non-analytic part where the latter is related to phase transitions and critical phenomena [15]. Accordingly, the EoS formulated in terms of the entropy density is given through  $s = s_a + s_n$ . Here, the an-

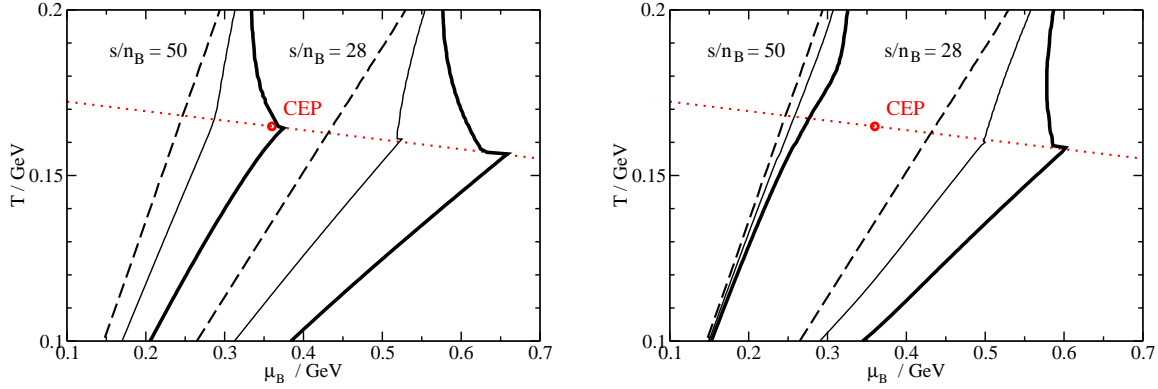


Fig. 2: Isentropic trajectories of the toy model (4) depending on the strength parameter  $A$  for  $s/n_B = 50, 28$ . Dashed, thin and solid lines exhibit results for  $A = 0., 0.5, 1.0$  respectively. Dotted lines represent the tangent on the estimated (pseudo-) critical line at the CEP. Left panel:  $\Delta T = 100$  MeV,  $\Delta\mu_B = 200$  MeV,  $D = 0.15$ ; right panel:  $\Delta T = 10$  MeV,  $\Delta\mu_B = 10$  MeV,  $D = 0.06$ .

alytic contribution  $s_a$  has to be adjusted to the known EoS outside of the critical region. The non-analytic part  $s_n$  should embody the feature of being continuous left to the CEP (i. e. at small chemical potentials) whereas on the right (at large chemical potentials) it generates a first order phase transition. A convenient parametrization of  $s_n$  for the 3D Ising model characterized by a set of critical exponents is given in [16]. Still, the corresponding variables employed usually in condensed matter physics including the order parameter need to be mapped into the  $T - \mu_B$  plane in the vicinity of the CEP. Details of this mapping and a useful formulation of the entropy density contribution can be found in the pioneering work [17] we rely on. In the following, we estimate the phase border line to be given by  $T_c(\mu_B) = T_c \left(1 + \frac{1}{2}d(\mu_B/3T_c)^2\right)$  with  $d = -0.122$  according to [1, 3] and locate the CEP at  $\mu_{B,c} = 360$  MeV in agreement with [4].

As a simple toy model, let us employ the first terms in (1), however, with constant expansion coefficients. The entropy density contributions are given by

$$s_a(T, \mu_B) = 4\bar{c}_0 T^3 + \frac{2}{9}\bar{c}_2 \mu_B^2 T, \quad s_n(T, \mu_B) = \frac{2}{9}\bar{c}_2 \mu_B^2 T A \tanh(S_c(T, \mu_B)) \quad (4)$$

with  $\bar{c}_0 = (32 + 21N_f)\pi^2/180$ ,  $\bar{c}_2 = N_f/2$  and  $N_f = 2$ .  $n_B$  follows from (4) via standard thermodynamic relations (cf. [17]) with integration constant  $n_B(0, \mu_B) = \frac{4}{3}\bar{c}_4(\mu_B/3)^3$  where  $\bar{c}_4 = N_f/4\pi^2$ . The ansatz for  $s_n$  has been chosen such that  $s_n \rightarrow 0$  for  $T \rightarrow 0$  and the net baryon density vanishes at  $\mu_B = 0$ . The parameter  $A$  describes the strength of the non-analytic contribution in the EoS. We apply the same  $S_c(T, \mu_B)$  as in [17] assuming a fairly large critical region parametrized by  $\Delta T = 100$  MeV,  $\Delta\mu_B = 200$  MeV and a stretch factor  $D = 0.15$ . Hence, CEP effects on the EoS and in particular on isentropic trajectories  $s/n_B = \text{const}$  in the  $T - \mu_B$  plane can be demonstrated. In Fig. 2, the influence of the strength parameter  $A$  on the behaviour of isentropic trajectories is exhibited. For increasing  $A > 0$ , the trajectories for large  $s/n_B$  tend to be attracted towards larger  $\mu_B$  due to the presence of the CEP. In fact, the CEP acts as an attractor on trajectories on the left whereas on the right a repulsive impact is found. Evidently, the curves on the right side of the CEP display the existence of the first order phase transition. By shrinking the critical region to  $\Delta T = 10$  MeV,  $\Delta\mu_B = 10$  MeV and  $D = 0.06$ , the influence of the CEP decreases (right panel of Fig. 2) in comparison with the results obtained for a large critical region (left panel of Fig. 2). In particular, the sections on the hadronic side become less affected when decreasing the extension of the critical region.

The parameters in the non-analytic entropy density contribution and in particular  $A$  have to be chosen such that standard thermodynamic consistency conditions are satisfied [17]. Accordingly, during the adiabatic expansion of the system and its related cooling, both  $n_B$  and  $s$  must decrease. For  $A < 0$

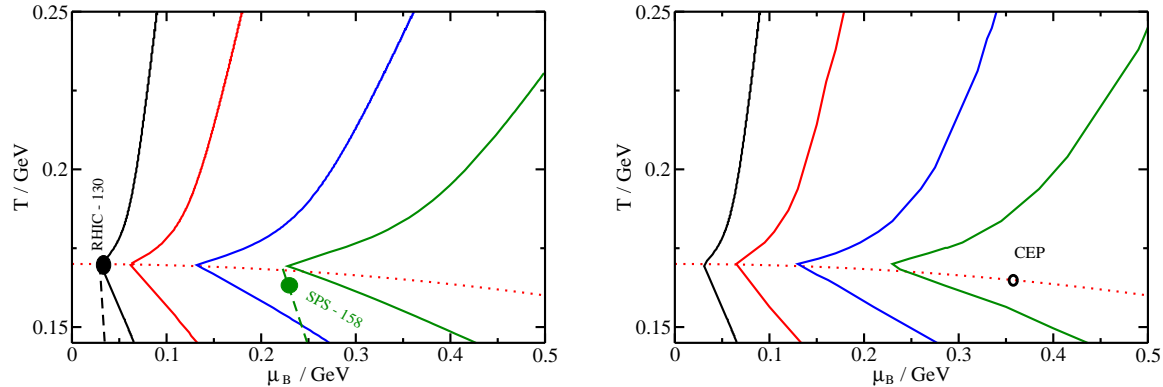


Fig. 3: Isentropic trajectories in the truncated quasi-particle model adjusted to lattice QCD [7, 8] without CEP (left panel) and with CEP effects included (right panel) parametrized by  $\Delta T = 10$  MeV,  $\Delta\mu_B = 10$  MeV,  $D = 0.06$  and  $A = 0.5$  for  $s/n_B = 200, 100, 50, 33$  (from left to right). Dotted line represents the estimated phase border line, long-dashed lines in the left panel depict resonance gas trajectories with corresponding chemical freeze-out points from [18].

with trajectories for large  $s/n_B$  bent to smaller  $\mu_B$  due to the CEP inclusion, however, these conditions are violated in the vicinity of the first order transition line. Therefore, the pattern of the isentropic trajectories as exhibited in Fig. 2 seems to be generic (cf. [17] for a different model with CEP which involves a hadronic low-temperature and a partonic high-temperature phase). Clearly, this statement decisively depends on  $s$  in the hadronic phase where the simple toy model cannot account for QCD.

In contrast, being inspired by lattice QCD we construct the EoS as truncated Taylor series expansion including the coefficients  $c_{0,2,4,6}(T)$  of Fig. 1. These lattice based trajectories are shown in Fig. 3 (left panel) where the pattern differs notably from the observations made in the above toy model. Although first principle evaluations still suffer from too heavy quark masses and deviate consequently from the resonance gas trajectories in the low-temperature phase, the values  $s/n_B$  on these lattice QCD deduced curves agree with the values at the according nearby chemical freeze-out points inferred from data [18]. Furthermore, in the deconfined phase lattice results are trustable due to convergence radius studies [8] at least up to  $\mu_B = 300$  MeV. Therefore, adjusting the analytic contribution of the EoS known from the lattice data by our quasi-particle model, critical end point effects should become visible only for larger  $\mu_B$  implying a small critical region. We include the CEP in line with the procedure outlined above in our quasi-particle model replacing  $\bar{c}_2$  by  $c_2(T)$  in  $s_n$  and considering a small critical region characterized by  $\Delta T = 10$  MeV,  $\Delta\mu_B = 10$  MeV and  $D = 0.06$  with strength parameter  $A = 0.5$ . As exhibited in Fig. 3 (right panel), CEP effects on isentropic trajectories are significant only for large  $\mu_B$  with negligible impact on the hadronic sections. Nonetheless, the baryon number susceptibility  $\chi_B = \partial^2 p / \partial \mu_B^2$  being a measure for baryon number fluctuations diverges for  $\mu_B > \mu_{B,c}$  (Fig. 4 right panel) due to the discontinuity evolving in  $n_B$  in contrast to the analytic behaviour (Fig. 4 left panel) stemming from the quasi-particle model not containing CEP effects.

## 4 Conclusion

Our quasi-particle model without implemented CEP was successfully compared with recent lattice QCD results of the Taylor series expansion coefficients  $c_0(T)$  and  $c_{2,4,6}(T)$ . Accordingly, our extrapolation procedure into the finite chemical potential region was tested. We considered simple models including phenomenologically the QCD critical end point and studied the effects on isentropic trajectories. We followed [17] and looked for indications of the CEP acting generically as attractor or repulsor. In fact, this is of interest with respect to the question whether CEP effects show up in heavy ion experiments only

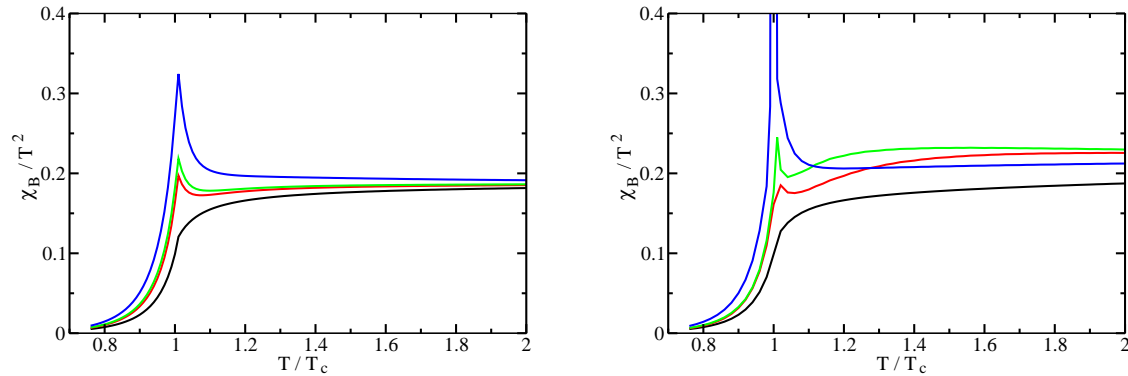


Fig. 4: Scaled baryon number susceptibility of the quasi-particle model neglecting  $c_6(T)$  without CEP (left panel) and with CEP inclusion (right panel) as function of  $T/T_c$  for  $\mu_B = 450, 330, 300, 150$  MeV (from top to bottom).

in a very narrow beam energy range. Clearly, appropriate dynamical simulations are needed to account properly for such questions. The study of the pattern of isentropic trajectories is only a first step towards elucidating possible implications of the very existence of the CEP in QCD.

Inspiring discussions with M. Asakawa and F. Karsch are gratefully acknowledged. The work is supported by BMBF, GSI, EU-I3HP.

## References

- [1] C. R. Allton et al., Phys. Rev. D **66** (2002) 074507
- [2] Ph. de Forcrand and O. Philipsen, Nucl. Phys. B **642** (2002) 290
- [3] Ph. de Forcrand and O. Philipsen, Nucl. Phys. B **673** (2003) 170
- [4] Z. Fodor and S. D. Katz, JHEP 0203 (2002) 014, JHEP 0404 (2004) 050
- [5] M. A. Halasz et al., Phys. Rev. D **58** (1998) 096007
- [6] M. Stephanov, Prog. Theor. Phys. Suppl. **153** (2004) 139 and references therein
- [7] F. Karsch, E. Laermann and A. Peikert, Phys. Lett. B **478** (2000) 447
- [8] C. R. Allton et al., Phys. Rev. D **68** (2003) 014507, Phys. Rev. D **71** (2005) 054508
- [9] C. Schmidt et al., Nucl. Phys. Proc. Suppl. **119** (2003) 517
- [10] R. V. Gavai and S. Gupta, Phys. Rev. D **71** (2005) 114014
- [11] F. Karsch, E. Laermann and C. Schmidt, Phys. Lett. B **520** (2001) 41
- [12] M. Asakawa, U. Heinz and B. Müller, Phys. Rev. Lett. **85** (2000) 2072 and references therein
- [13] A. Peshier et al., Phys. Rev. D **54** (1996) 2399, Phys. Rev. C **61** (2000) 045203, Phys. Rev. D **66** (2002) 094003
- [14] M. Bluhm, B. Kämpfer and G. Soff, Phys. Lett. B **620** (2005) 131
- [15] W. Gebhardt and U. Krey, *Phasenübergänge und kritische Phänomene*, Friedr. Vieweg & Sohn, Braunschweig/Wiesbaden (1980)

- [16] R. Guida and J. Zinn-Justin, Nucl. Phys. B **489** (1997) 626
- [17] C. Nonaka and M. Asakawa, Phys. Rev. C **71** (2005) 044904
- [18] F. Becattini et al., Phys. Rev. C **69** (2004) 024905